Optimal Sizing of Battery Energy Storage Systems for Small Modular Reactor based Microgrids

Xuebo Liu[1], Molly Ross[2], Hitesh Bindra[2], and Hongyu Wu[1]
1 The Mike Wiegers Department of Electrical and Computer Engineering
2 The Alan Levin Department of Mechanical and Nuclear Engineering
Kansas State University, Manhattan, Kansas, 66502, USA

***Abstract*—Battery energy storage systems (BESS) are increasingly deployed in microgrids due to their benefits in improving system reliability and reducing operational costs. Meanwhile, advanced small modular reactors (SMRs) offer many advantages, including relatively small physical footprints, reduced capital investment, and the ability to be sited in locations not possible for larger nuclear plants. In this paper, we propose a bi-level operational planning model that enables microgrid planners to determine the optimal BESS size and technology while taking into account the optimal long-term (a yearly simulation with a 15-min resolution) operations of a microgrid with SMRs and wind turbines. Case studies are performed using realistic BESS and grid data for two BESS technologies, i.e., Li-Ion battery and compressed air energy storage. Numerical results show the effectiveness of the proposed bi-level model. The pros and cons of the two BESS technologies are also revealed.**

NOMENCLATURE

Indices, Sets, and Parameters

NT Total number of operational time periods
t Index of operational time periods, t=1,2,3,...,NT
LT Total number of years in BESS lifetime
PW Present worth factor
y Index of years, y=1,2,3,...,LT
Cap Capacity of BESS
$EC^{\max}$ Max allowable daily electricity cost
τ Time interval, in hour
$E^{\max}$ Max accumulative energy from the grid
$C^{\max}/D^{\max}$ Maximum charge/discharge rate of BESS
$SOC^{\min}/SOC^{\max}$ Min/Max state of charge (SOC) for BESS
η^C/η^D Charging/discharging efficiency of BESS
$\bar{\lambda}_t$ Electricity price at time t
$\bar{P}_t^W$ Wind generation at time t
$\bar{P}_t^D$ Electricity demand at time t

Variables

OC_y^{NB} Annual operating cost without BESS at year y
OC_y^B Annual operating cost with BESS at year y
∂_y Battery degradation coefficient at year y
OM_y Operation and maintenance cost of BESS at year y
IC Up-front capital cost of BESS
I_t^C/I_t^D Charging/discharging indicator of BESS at time t; 1 for charge/discharge, otherwise 0
P_t^N Power generated by SMR at time t
P_t^B Electricity consumption/generation by BESS at time t
P_t^G Power extracted/injection from/to grid at time t
SOC_t SOC of at time t

I. INTRODUCTION

The deployment of battery energy storage systems (BESS) in electric distribution networks such as microgrids has significantly increased in recent years. Deploying BESS in the context of microgrids can provide a variety of grid services to improve reliability, resiliency, and economic gains. A microgrid is defined as a group of interconnected loads and distributed energy resources (DERs) with clearly defined electrical boundaries that act as a single controllable entity with respect to the grid and can connect and disconnect from the grid to enable it to operate in both grid-connected and islanded modes [1]. BESS is an essential component in a microgrid and plays a critical role in both modes. BESS, through demand response, could provide additional operational flexibilities for microgrids operated in either a grid-connected or islanded mode [2]. In the isolated mode, BESS is typically utilized to regulate the system frequency and voltage by either charging or discharging when a generation-demand mismatch occurs to maintain the stability of the microgrid (e.g., voltage and frequency). In the grid-tied mode, the BESS reduces the microgrid operation cost by efficiently utilizing renewable generation and taking advantage of electricity price variations. Meanwhile, advanced small modular reactor (SMR) is a promising type of nuclear reactors that can generate from tens of megawatts up to hundreds of megawatts via modular technology to achieve that purchasing economies of series production and short construction times [3]. It demonstrates superiority such as reducing footprints, capital investment, and safely developing [4].

BESS deployment in microgrids has been extensively studied in the literature [5]. The work conducted in this area can be divided into two main topics: BESS planning and operation. The main objective of BESS planning is to determine the optimal BESS size. Besides the optimal size, some of the existing studies investigate the optimal BESS technology and location. From the standing point of BESS operation, the focus is on proposing control and scheduling approaches to manage BESS operation to achieve a specific objective. However, the size of the BESS is the most important factor determining the ability to deliver the desired economic and technical benefits. The microgrid-integrated BESS planning and operation with heterogeneous DERs (e.g., SMR, renewable generation) is still an open and pressing issue.

2021 IEEE Kansas Power and Energy Conference (KPEC) | 978-1-6654-4119-3/21/$31.00 ©2021 IEEE | DOI: 10.1109/KPEC51835.2021.9446203

978-1-6654-4119-3/21/$31.00 ©2021 IEEE

This paper addresses this issue by systematically coupling BESS with SMR generation, distributed wind turbines, electricity demand, and electricity prices in a microgrid. We propose a bi-level operational planning model that enables microgrid planners to determine the optimal BESS size and technology while taking into account the optimal long-term (hourly scheduling in an entire year) operations of a microgrid with SMRs and wind turbines. Case studies are performed using most-up-to-date specifications and data for two BESS technologies, i.e., Li-Ion battery and compressed air energy storage (CAES). The remainder of this paper is structured as follows. The proposed BESS sizing method and formulation are described in Section II. Numerical results are conducted and analyzed in Section III. Section IV concludes the paper.

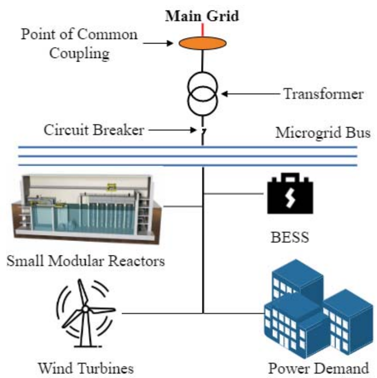

Fig. 1. Schematic of Small Modular Reactors based microgrid with DERs

II. Microgrid-integrated BESS Sizing

Figure 1 demonstrates the schematic of the SMR-based microgrid with BESS and distributed wind energy. A BESS is normally sized based on its power rating and energy rating. The power rating is defined as the rate with which the BESS can supply energy while the energy rating indicates the maximum amount of energy that can be delivered to the demand at each cycle [6]. We apply a cost-based sizing method, in which we size the BESS to maximize the total benefits associated with installing the BESS in the microgrid, while considering nuclear safety.

A. Reactor power constraints

Due to safety constraints with thermal cycling and xenon poisoning, as well as economic constraints due to the large fixed costs of operating a nuclear power plant, it is not feasible to have nuclear power meet the entire grid demand not accounted for by wind. While the limitations for flexible operation are slightly different for each reactor design, there are some general guidelines that have been advised from various governing bodies. This work used guidelines put forth by the European Utilities Requirements, as shown in Table I [7]. These guidelines include limitations for flexible operation for both normal operation and emergency operation, however we only considered the limitations for normal operation.

TABLE I
EUR regulations on LWRs operating in load following mode

Power change Regime	Max Ramp Rate	Max Cycles
$50\% to 100\%$	$\pm 5\% P_r$/min	20,000
Within $\pm 10\% P_r$	$\pm 5\% P_r$/sec	No Limit
Within $\pm 20\% P_r$	$\pm 10\% P_r$/min	20,000

Without any form of energy storage, this microgrid would rely entirely on nuclear power to account for the discrepancy between power demand and wind power production. This would almost always result in the reactor operating outside of safe, allowable ramp rate limits. In order to operate the reactor within safe limits, the fluctuations in power had to be reduced. To limit these fluctuations, the wind power was modelled using the (Ornstein-Uhlenbeck) OU process, a Langevin equation, which separates the stochastic series into stochastic and deterministic parts. The OU process is defined by the stochastic differential equation in Equation 1, where x is the modeled stochastic process, θ is the drift or deterministic term, σ is the diffusion or stochastic term, and η is a white noise term.

$$\frac{dx}{dt} = -\theta x + \sigma \eta(t) \tag{1}$$

The nuclear power was calculated as the grid load minus the OU modeled wind power. The parameters of the OU process were then calculated from the wind power data. The stochastic term, σ, was then reduced, a new wind power time series was generated from the OU process, and the resulting required nuclear power from this OU generated wind power was calculated. This process was repeated until the magnitude of the stochastic fluctuations in wind, and thus nuclear power, allowed the nuclear plant to operate within the EUR guidelines. The remaining power not accounted for by wind or nuclear must then be generated from another source, in this case energy storage.

B. BESS Sizing Method

The investment cost associated with purchasing, installing, operating, and maintaining of the BESS is greatly related to their size. The installation of the BESS is economically justifiable only if the provided economic benefits outweigh the investment cost. We formulate the BESS sizing problem as an optimization problem whose objective is to maximize the total BESS benefits (i.e., a cost-benefit analysis). We consider the BESS size as a design variable whose optimal value is determined by solving a series of optimization problems. Specifically, an iterative-based method is proposed, in which the steady-state microgrid optimal operation problem is solved for different BESS sizes within the predetermined minimum and maximum values. Figure 2 shows the flowchart of the proposed BESS sizing while considering its long-term operation. The BESS sizing problem is firstly decomposed into an upper-level master problem, in which the BESS size is chosen as a fixed value, and a lower-level subproblem in which the BESS operating cost is simulated and calculated within its lifetime

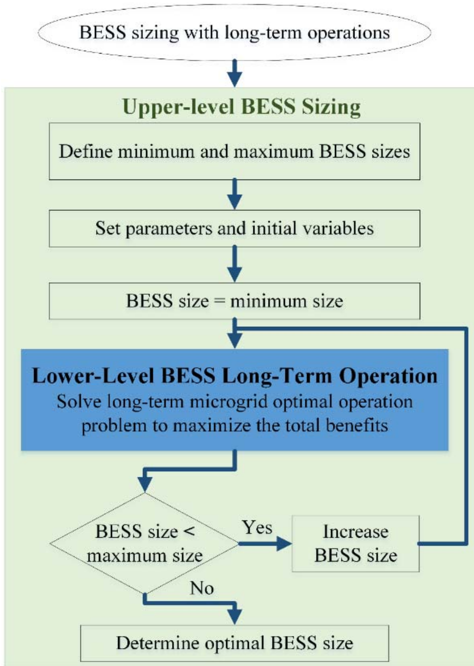

Fig. 2. Flowchart of the proposed bi-level BESS sizing

(long-term operation), as shown in Fig.2. The BESS size is then updated and the process is repeated until all size options are traversed. Finally, the BESS optimal size is chosen as the one with the maximal benefits. In order to capture the true benefits of the BESS in long-term operations, unlike previous studies where BESS operations on a number of representative days or weeks are studied, we conduct here yearly simulations of the microgrid operation with a 15-minute resolution (i.e., 4*24*365=35,040 data points a year) for each of the BESS size chosen.

C. Problem and Formulation

We consider both grid-connected and islanded operation modes, in which the solution of the BESS sizing problem will return the optimal BESS size together with the microgrid optimal schedules that minimize the total microgrid cost. The long-term BESS operation in its lifetime is taken into consideration when the optimization problem is solved. The upper-level sizing problem is formulated as a Markov Decision Process (MDP) problem with the following objective function:

$$Max \quad \sum_{y=1}^{LT} PW \cdot [(OC_y^{NB} - OC_y^{B}) - OM_y] - IC \tag{2}$$

where PW is the present worth factor calculated based on the discount and inflation rates; IC is the investment cost consisting of capital costs for all battery systems are presented for battery capital and management systems (expressed in terms of \$/kWh), the balance of plant (BOP) (\$/kW), power conversion systems (PCS) (\$/kW), and construction and commissioning (C&C) (\$/kWh); OM_y is assumed to be fixed over the BESS lifetime as long as the battery size if determined. The lower-level annual microgrid operation with BESS is formulated as mixed-integer linear programming (MILP) problem with the objective as follows:

$$OC_y^{(\cdot)} = argmin \ \sum_{t=1}^{NT} \tau \cdot P_t^G \cdot \bar{\lambda}_t \tag{3}$$

In (3), the microgrid can participate in a demand-response program or other ancillary services. Time-based pricing schemes, including dynamic and time-of-use pricing, could be applied to the MILP optimization model. Both microgrid-wide and generator-level constraints are included in the formulation as follows:

1) Constraints associated with Microgrid: The microgrid-wide constraints are listed in (4)–(7). Constraint (4) guarantees that the electricity generation and load are balanced at time t, where P_t^G is positive when the house extracts electricity from the grid and negative when the house injects electricity into the grid. Here, the scheduled power consumption/generation at each time interval is the average value during a given time interval. Constraint (5) ensures that the maximum electricity extracted from the grid at any given time period should not exceed a specified value. This constraint is suitable for microgrid customers who enroll in a demand-response program in response to utilities' power-reduction requests during critical time periods. Constraint (6) shows that the total electricity energy cost does not exceed a threshold, which may be prescribed by the microgrid customers. This type of constraint provides the customer with more restrictive control of their daily energy cost. Constraint (7) indicates that the total energy drawn from the grid should not exceed a predefined value. A zero-energy microgrid can be modeled by setting $E^{\max}$ in a long-term operation, indicating that the total energy consumption is equal to the energy generated by the local on-site RES:

$$P_t^G + P_t^N + \bar{P}_t^W = \bar{P}_t^D + P_t^B, \ \forall t \tag{4}$$

$$P_t^G \leq P_t^{\max}, \forall t \tag{5}$$

$$\sum_{t=1}^{NT} \hat{\lambda}_t \cdot P_t^G \cdot \tau \leq EC^{\max}, \tag{6}$$

$$\sum_{t=1}^{NT} p_t^G \cdot \tau \leq E^{\max} \tag{7}$$

2) Battery Energy Storage Constraints: The residential battery constraints include charge/discharge rate limits, state of charge (SOC) dynamics, SOC limits, and limits on initial/final SOC [8],[9],[10], which are given in (8)–(13), respectively. In (8) and (9), the BESS power is positive when charging, negative when discharging, and 0 when the storage is idling. In (11), α is the battery degradation parameter on the capacity fade, which is defined using a linearized depth of discharge versus life-cycle curve [5]. Constraint (13) suggests that the storage follows a daily cycle when the SOC at the last period ($t = NT$) would be equal to that of the initial time in the scheduling horizon ($t = 0$):

$$0 \leq P_t^B \leq I_t^C \cdot C^{Max}, \forall t \tag{8}$$

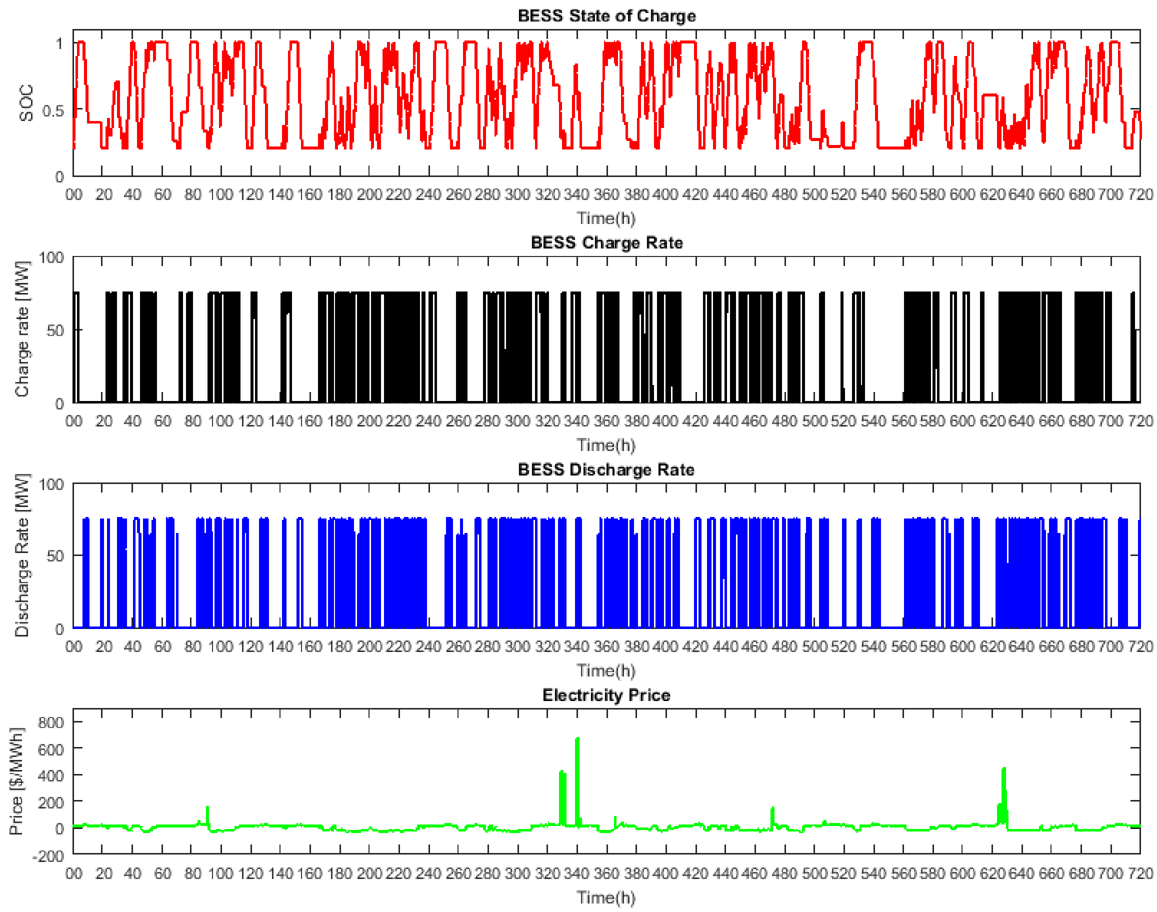

Fig. 3. Monthly schedules of the Li-Ion battery sized at 30MWh/7.5MW

$$-D^{Max} \cdot I_t^D \leq P_t^B \leq 0, \forall t \tag{9}$$

$$I_t^C + I_t^D \leq 1, \forall t \tag{10}$$

$$\underset{\forall t}{SOC_t} = \begin{cases} SOC_{t-1} + P_t^B \cdot \eta^C / Cap \cdot \alpha, \ P_t^B \geq 0 \\ SOC_{t-1} + P_t^B / \eta^D / Cap \cdot \alpha, \ P_t^B < 0 \end{cases} \tag{11}$$

$$SOC^{\min} \leq SOC_t \leq SOC^{\max}, \ \forall t \tag{12}$$

$$SOC_0 = SOC_{NT} \tag{13}$$

III. Numerical Results

We use one-year historical datasets from March 1st 2018 to Feb, 28th 2019 from the Electric Reliability Council of Texas (ERCOT) for wind generation, electricity demand, and electricity prices (i.e., locational marginal prices) for the yearly simulation. The SMR parameters are from [11]. The datasets have a time resolution of 15 minutes, totaling 35,040 data points of the wind, demand, and electricity prices. In the simulation, we choose Li-Ion battery with a 10-year lifetime and CAES with a 25-year lifetime at different sizes. For simplicity, we duplicate the datasets over the years within the BESS's lifetime. However, a growth rate on demand and wind capacity can also be used. Here, Li-Ion battery costs and efficiency parameters under energy to power ratio of 4.0 are extracted from [12]. The minimum SOC is set to 20% to minimize its battery degradation. Both the inflation and discount rates are assumed to be 2.1% in the battery's lifetime. We do not consider federal or state incentives in our simulation. The lower-level MILP formulation for the long-term microgrid operation is coded in the General Algebraic Modeling System (GAMS) using a CPLEX solver [13], while the upper-level BESS sizing problem is implemented in MATLAB.

Figure 3 shows a monthly schedule of a Li-Ion battery sized at 30MWh/7.5MW. As seen, in order to maximize the economic benefit of the microgrid, the battery is charged when the electricity price is relatively low and is discharged when the electricity price is high. It is always charged at the maximum charge power when the price is below zero and discharged at the maximum discharge power when the price spikes occur. Additionally, the Li-Ion battery completes more than 33 cycles during this month. Figure 4 shows a monthly schedule of the CAES sized at 30MWh/1.875MW. Compared with the Li-Ion battery, the CAES behaves similarly in terms of charging and discharging with respect to the electricity price; however, it has much fewer cycles due to its lower round-trip

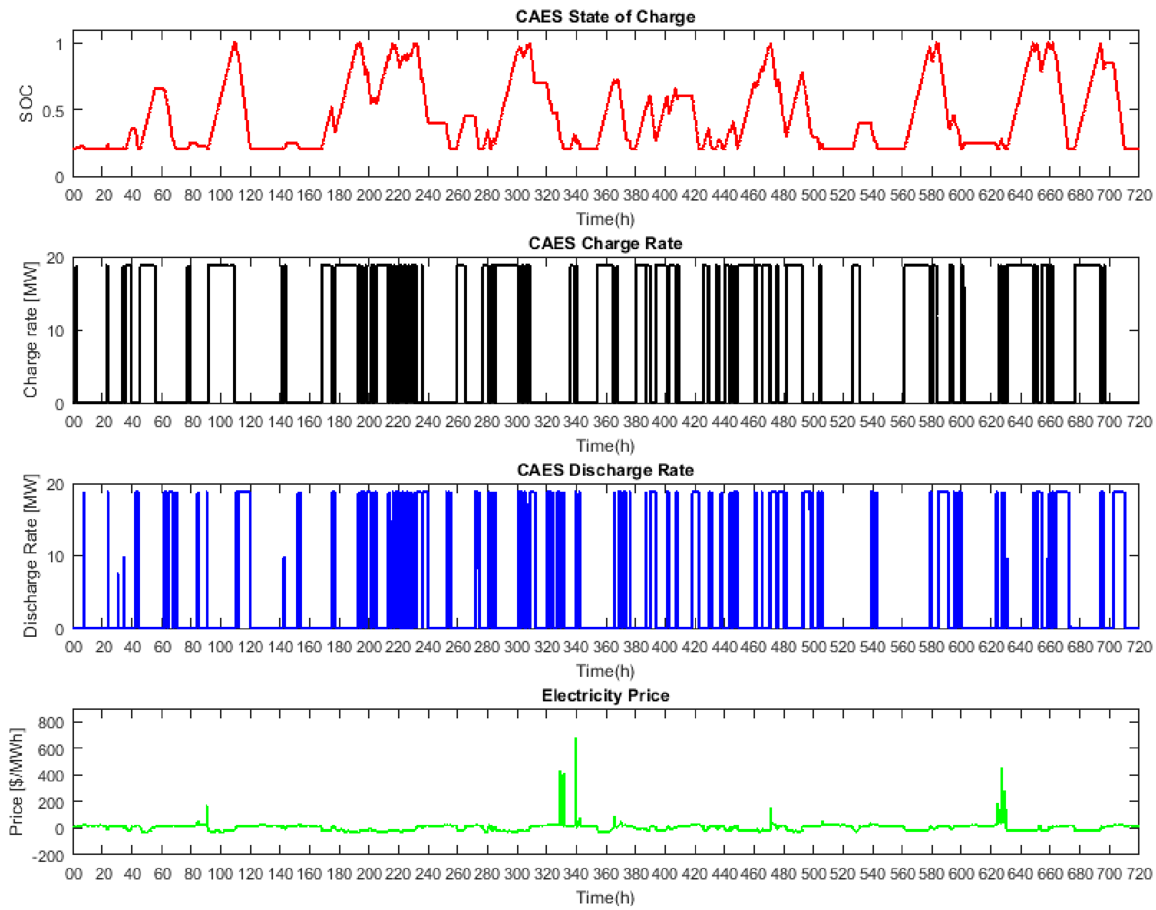

Fig. 4. Monthly schedules of the CAES sized at 30MWh/1.875MW

efficiency.

Microgrid annual operating cost and net benefit versus storage size ranging from 10 MW to 60 MW are listed in Table II, in which a negative operating cost indicates a profit the microgrid gains by selling electricity to the utility grid. The last row with zero energy and zero power in Table II represents the microgrid operating cost without installing any energy storage. As expected, larger-size storage will lead to a higher annual net benefit (the difference between with and without storage) in the microgrid operation. However, the high annual net benefit is generated at the cost of massive capital investment cost and high O&M cost of the Li-ion battery.

TABLE II
MICROGRID ANNUAL OPERATING COST AND NET BENEFIT VERSUS LI-ION BATTERY SIZES

Energy (MWh)	Power (MW)	Operating cost w/ BESS ($)	Net benefit w/ BESS ($)
60	15	-978,413	995,800
50	12.5	-812,358	829,744
40	10	-645,034	662,421
30	7.5	-480,299	497,685
20	5	-314,468	331,854
10	2.5	-148,259	165,646
0	0	17,386	0

TABLE III
LIFETIME BENEFITS OF DIFFERENT STORAGE TECHNOLOGIES

Energy (MWh)	Lifetime benefit ($)	
	Li-Ion, 4 E/P 10-year lifetime	CAES, 16 E/P 25-year lifetime
60	-20,130,128	-1,875,132
50	-16,775,951	-1,563,108
40	-13,433,889	-1,248,522
30	-10,067,111	-936,124
20	-6,710,797	-626,734
10	-3,358,084	-319,507

Table III shows the lifetime benefits of two storage technologies, i.e., Li-Ion battery and CASE. In Table III, which the lifetime benefit is calculated base on the capital cost, O&M cost (fixed plus variable), and net benefit during the lifetime of each technology. It is seen that the lifetime benefit of the current state-of-the-art Li-Ion battery is negative at today's electricity price, indicating that installing a Li-Ion battery in this microgrid does not make economic sense if no other incentives (tax credit) are in place. With the advance in Li-Ion battery technology, one would expect a much longer lifetime and lower capital cost per MWh for the Li-Ion battery to make economic sense. A 50% lifetime increase and a 50% capital cost reduction will make the lifetime benefit of the Li-Ion battery positive in our simulations. In Table III, CAES has a much higher lifetime benefit (still negative), in contrast to the Li-Ion battery, which is attributed to its much longer lifetime and significantly lower capital cost. Therefore, CAES might be a better choice for the microgrid studied in this paper.

IV. Conclusion

This paper proposes a bi-level operational planning model to determine the optimal BESS size and technology while taking into account the optimal long-term (hourly scheduling in an entire year) operations of a microgrid with SMRs and wind turbines. We compare two different technology, i.e., Li-Ion and CAES, while taking into accounting SMR and wind power for maximizing the efficiency of a microgrid. Comparative simulation results show that the CAES is a superior energy storage technology for the specific SMR-based microgrid since it has a longer technology lifetime. Our future work will use other optimization methods, such as approximate dynamic programming while considering solar and ammonia production in an agricultural microgrid.

V. ACKNOWLEDGEMENT

This material is based upon work supported by the U.S. National Science Foundation under Grant No. 1856084 for the FEWtures project.

References

[1] Department of Energy Office of Electricity Delivery and Energy Reliability., "2012 microgrid workshop report," p. 33.

[2] L. Che, M. Khodayar, and M. Shahidehpour, "Only connect: Microgrids for distribution system restoration," *IEEE Power and Energy Magazine*, vol. 12, no. 1, pp. 70–81.

[3] Small nuclear power reactors - world nuclear association. [Online]. Available: https://www.world-nuclear.org/information-library/nuclear-fuel-cycle/nuclear-power-reactors/small-nuclear-power-reactors.aspx

[4] Advanced small modular reactors (SMRs). [Online]. Available: https://www.energy.gov/ne/nuclear-reactor-technologies/small-modular-nuclear-reactors

[5] "State-of-the-art in microgrid-integrated distributed energy storage sizing," vol. 10.

[6] J. M. Eyer and G. P. Corey, "Energy storage for the electricity grid : benefits and market potential assessment guide : a study for the doe energy storage systems program." 2 2010. [Online]. Available: https://www.osti.gov/biblio/1031895

[7] A. Lokhov, "Technical and economic aspects of load following with nuclear power plants," *NEA, OECD, Paris, France*, 2011.

[8] H. Wu, A. Pratt, and S. Chakraborty, "Stochastic optimal scheduling of residential appliances with renewable energy sources," in *2015 IEEE Power Energy Society General Meeting*, 2015, pp. 1–5.

[9] A. Pratt, D. Krishnamurthy, M. Ruth, H. Wu, M. Lunacek, and P. Vaynshenk, "Transactive home energy management systems: The impact of their proliferation on the electric grid," *IEEE Electrification Magazine*, vol. 4, no. 4, pp. 8–14.

[10] X. Liu, H. Wu, L. Wang, and M. N. Faqiry, "Stochastic home energy management system via approximate dynamic programming," *IET Energy Systems Integration*, vol. 2, no. 4, pp. 382–392.

[11] J. Edwards, D. Franken, H. Bindra, and P. Sabharwall, "Packed bed thermal storage for compact light water-cooled small modular reactors," *Transactions of the American Nuclear Society*, vol. 115, no. 1, pp. 981–984.

[12] K. Mongird, V. V. Viswanathan, P. J. Balducci, M. J. E. Alam, V. Fotedar, V. S. Koritarov, and B. Hadjerioua, "Energy storage technology and cost characterization report," 7 2019. [Online]. Available: https://www.osti.gov/biblio/1573487

[13] ILOG CPLEX optimization studio - resource library. [Online]. Available: https://www.ibm.com/products/ilog-cplex-optimization-studio/resources